Lab on a Chip

Controlled Co-Precipitation of Biocompatible Colorant-Loaded Nanoparticles by Microfluidics for Natural Color Drinks

Journal:	*Lab on a Chip*
Manuscript ID	LC-ART-03-2019-000240.R1
Article Type:	Paper
Date Submitted by the Author:	01-May-2019
Complete List of Authors:	Kong, Linlin; Zhejiang University Chen, Ran; Zhejiang University, Department of Energy Engineering Wang, Xingzheng; Department of Energy Engineering, Zhejiang University Zhao, Chun-Xia; The University of Queensland, Australian Institute for Bioengineering and Nanotechnology Chen, Qiushui; Tsinghua University, Chemistry Hai, Mingtan; Harvard University Chen, Dong; Zhejiang University, Chemical and Biological Engineering; University of Colorado at Boulder, Physics Yang, Zhenzhong; Chinese Academy of Sciences Weitz, David; Harvard University, Department of Physics

PAPER

Controlled Co-Precipitation of Biocompatible Colorant-Loaded Nanoparticles by Microfluidics for Natural Color Drinks

Received 00th January 20xx,
Accepted 00th January 20xx

DOI: 10.1039/x0xx00000x

Linlin Kong,[a†] Ran Chen,[a,b†] Xingzheng Wang,[a] Chun-Xia Zhao,[b,c] Qiushui Chen,[b] Mingtan Hai,[b] Dong Chen,*[a,b] Zhenzhong Yang*[b,d] and David A. Weitz*[b]

Natural colorants, which impart a vivid color to food and add additional health benefits, are favored over synthetic colorants; however, their applications are limited by their low solubility in water and low stability. Here, we develop a versatile microfluidic strategy to incorporate natural colorants in shellac nanoparticles with controlled physicochemical properties. The rapid mixing in the microfluidic channels ensures that the mixing time is shorter than the aggregation time, thus providing control over the co-precipitation of the colorant and the polymer. By introducing molecular interactions, colorant nanoaggregates are efficiently embedded in the polymer matrix, forming hierarchical colorant-loaded nanoparticles. The colorant-loaded nanoparticles dispersed in water are transparent and stable over a wide pH range and their polymer matrix also provides a favorable microenvironment that greatly improves the shelf life of the colorants. The improved solubility, stability and bioavailability of the natural colorants suggest that shellac nanoparticles are ideal carriers and the stable, transparent dispersions of biocompatible colorant-loaded nanoparticles in water are well-suited for the development of functional foods, such as natural color drinks.

Introduction

Color is one of the most important visual attributes of food and is directly related to the perception of food quality.[1] Synthetic dyes are usually added to foods to improve their appearance; however, these dyes may results in health issues such as irritation, intolerance and carcinogenicity.[2] Natural colorants, that not only impart color but also have well-documented health benefits, are preferred for food coloring as a consequence of perceived consumer preference as well as legislative action.[3] However, natural colorants are generally hydrophobic and sensitive to light, temperature, pH and redox agents, which severely limits their applications.[4] Curcumin (diferuloylmethane, the principal curcuminoid of turmeric), for example, is a yellow natural colorant[5] and has wide-range beneficial properties, such as antioxidant, anti-inflammation and anti-carcinogen.[6-9] However, these benefits are limited by its low bioavailability due to its poor solubility in water (~11 ng/mL) and low stability.[10,11] Therefore, replacement of synthetic colors with natural alternatives remains an important challenge and it is highly desired to develop a biocompatible preparation using all FDA-approved materials that improve natural colorants' solubility, stability and bioavailability.

Nanoparticles that encapsulate hydrophobic natural colorants, disperse them in water, control their release, protect them from ambient conditions and improve their stability can effectively alleviate the deficiencies of the natural colorants[12,13] and have become an attractive technology for a myriad of applications.[14,15] Various methods have been developed to prepare nanoparticles for encapsulation, such as spray drying, coacervation and nanoprecipitation.[16-19] Despite these significant advances, encapsulation of natural colorants in biocompatible nanoparticles and dispersion of them in water for applications of natural color drinks remain the most challenging problem. The system must meet several critical criteria at the same time: all FDA-approved components, transparent, stable against sedimentation, high encapsulation efficiency, maximum protection against degradation, low batch variation and easy to scale up. A simple preparation method that is suitable for direct oral administration hasn't been available yet and innovations of technologies and materials that entrap natural colorants using all FDA-approved materials for effective dispersion and protection are thus essential.

Microfluidics, which provides precise control and rapid mixing, has shown considerable promise in the development of novel nanoparticles with controlled size[20-22] and hierarchical structure.[23,24] For example, co-precipitation of natural colorants

[a] Institute of Process Equipment, College of Energy Engineering, Zhejiang University, Zheda Road No. 38, Hangzhou, 310027, China. E-mail: chen_dong@zju.edu.cn
[b] John A. Paulson School of Engineering and Applied Sciences, Harvard University, Cambridge, MA 02138, USA. E-mail: weitz@seas.harvard.edu
[c] Australian Institute for Bioengineering and Nanotechnology, The University of Queensland, St Lucia, QLD 4072, Australia.
[d] State Key Laboratory of Polymer Physics and Chemistry, Institute of Chemistry, Chinese Academy of Sciences, Beijing, 100190, China. E-mail: yangzz@iccas.ac.cn
† These authors contributed equally to this work.
Electronic Supplementary Information (ESI) available: This material is available free of charge *via* the Internet at http://pubs.acs.org. See DOI: 10.1039/x0xx00000x

and biocompatible polymers offers a simple and gentle way to fabricate colorant-loaded nanoparticles. However, conventional synthesis of these nanoparticles by bulk mixing typically lacks control over the mixing process and thus compromises the properties of the resulting nanoparticles.[25] In contrast, precise control and rapid mixing in microfluidics allow the better optimization of the nanoparticles' performances.[26,27] Therefore, the application of microfluidics in particle preparation offers a unique opportunity to develop biocompatible nanoparticles with desired properties, addressing the challenges encountered in the applications.

In this paper, we develop a simple, robust and reproducible microfluidic strategy to entrap hydrophobic natural colorants in biocompatible nanoparticles, which improve the dispersity, stability and bioavailability of the colorants. We rapidly mix the solution of curcumin and shellac in ethanol with water in a flow-focusing microfluidic device. Because the mixing time is shorter than the aggregation time, curcumin and shellac co-precipitate, forming a hierarchical structure of curcumin nanoaggregates in shellac nanoparticles. An extremely high encapsulation efficiency is achieved via the introduction of molecular interactions and the stability of curcumin is greatly improved due to the favorable microenvironment provided by the nanoparticles. Dispersion of these nanoparticles in water is readily edible, transparent, stable and colorful. The excellent performances of the resulting colorant-loaded nanoparticles show a great promise for their practical applications in natural drinks with appealing color and health benefits.

Materials and methods

Materials

Curcumin (from curcuma longa, powder; Sigma-Aldrich, United States) and chlorophyll (chlorophyll a from spinach; Sigma-Aldrich, United States) are the yellow and green food colorants, respectively. Shellac is employed as the encapsulant (wax free, tested according to Ph. Eur.; Sigma-Aldrich, United States). Food colorant and shellac are co-dissolved in ethanol (200 proof, anhydrous; Koptec, United States).

Sample preparation

3.5 mg curcumin is dissolved in 1 ml ethanol with 0 mg/ml, 10 mg/ml, 50 mg/ml and 100 mg/ml shellac, respectively. The polymer solution is used as the inner phase. Distilled water (Milli-Q system; Millipore Corporation, United States) is used as the outer phase. Glass capillary microfluidic device is fabricated by inserting tapered cylindrical capillaries into a square capillary (Atlantic International Technology, Inc., United States). All fluids are pumped into the microfluidic device using syringe pumps (Harvard PHD 2000 series; Harvard Apparatus, United States). When the polymer solution is flow-focused by water in the microfluidic channels, curcumin and shellac co-precipitate, forming curcumin-loaded shellac nanoparticles. Different color shades are obtained by subsequent dilutions. In bulk preparation, 100 μl of the polymer solution is quickly infused into a reservoir of 3 ml DI water using 1-200 μl gel-loading pipet tips. Chlorophyll is encapsulated in shellac nanoparticles following the same procedure.

Characterization of nanoparticles

The particle size and the zeta potential are measured using a Zetasizer (Nano series; Malvern). Infrared spectrums of shellac nanoparticles and curcumin-loaded nanoparticles are measured by a Perkin Elmer FT-IR (Spectrum ONE; Perkin Elmer). Scanning electron microscope (SEM) images are obtained using an Ultra55 Field Emission Scanning Electron Microscope (FESEM Ultra55; Carl Zeiss, United States). SEM samples are dried using a freeze dryer (VirTis AdVantage Plus EL-85; SP Scientific). UV-Vis absorption of curcumin is measured using a UV-Vis spectrophotometer (Cary 60 UV-Vis; Agilent Technologies).

Encapsulation efficiency and stability test

Encapsulation efficiency is defined as the fraction of initial curcumin that is encapsulated by shellac nanoparticles. Unencapsulated curcumin is left in the supernatant when curcumin-loaded nanoparticles aggregate and sink at pH=2 and its concentration is calculated by measuring the UV-Vis absorption, which is linearly proportional to the curcumin concentration. To test the stability, equal amounts of curcumin-loaded nanoparticles in separate vials are stored at 4°C and protected from light. After 29 days, they are moved to room temperature (25°C). The retention of curcumin in each vial is determined by its UV-Vis absorption at ~430 nm and is monitored at 0, 7, 14, 29, 36, 43 and 57 days. All measurements are performed in duplicate.

Cell cytotoxicity and cell bioavailability

Cell cytotoxicity of plain shellac nanoparticles is tested on HT-29 and CACO-2 cells. Cell viabilities of HT-29 and CACO-2 cells cultured in the presence of shellac nanoparticles with a concentration of 40 and 80 μM are determined at time points of 24, 48 and 72 hours. Cell bioavailability of curcumin loaded in shellac nanoparticles is tested on HT-29 and DLD1 cells. Cell viabilities of HT-29 and DLD1 cells cultured in the presence of curcumin-loaded shellac nanoparticles with a curcumin concentration of 5, 10, 20, 40 and 160 μM are determined after 6 hours' cell culture. HT-29, CACO-2 and DLD1 cells are purchased from ATCC (Manassas, VA)

Results and discussion

Preparation of biocompatible colorant-loaded nanoparticles for natural color drinks.

To prepare the colorant-loaded nanoparticles, we use curcumin as the model natural colorant and shellac, an FDA-approved natural resin, as the polymer matrix, whose chemical structures are shown in Fig. S1.[28,29] We dissolve curcumin and shellac together in ethanol and quickly mix the solution with water in a flow-focusing microfluidic device, as modelled in Fig. 1a and Fig. S2. In the microfluidic device, the solution of curcumin and

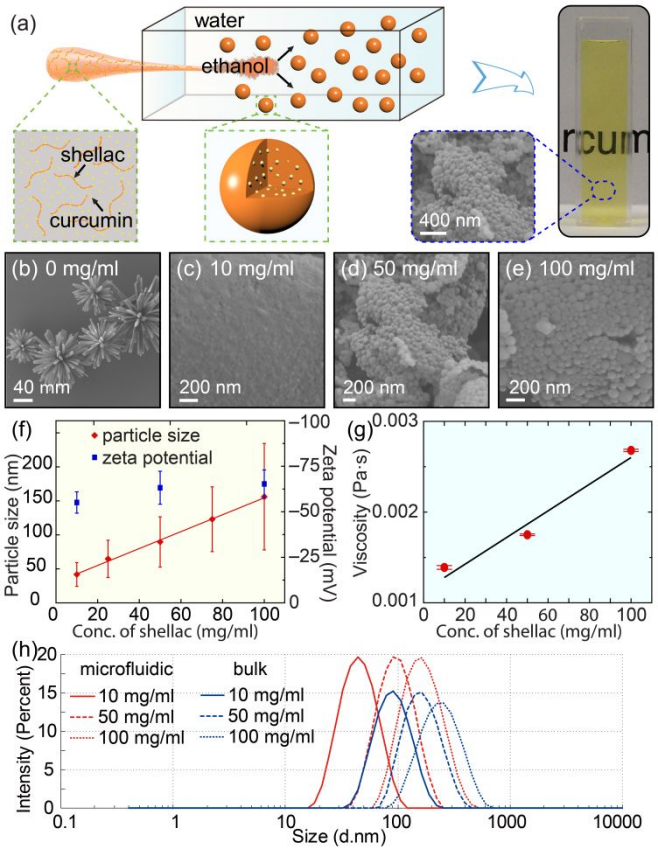

Fig. 1 Preparation of biocompatible colorant-loaded nanoparticles for natural color drinks. (a) Schematic illustration of curcumin-loaded shellac nanoparticles upon solvent diffusion and co-precipitation. SEM images of nanoparticles prepared using (b) 0 mg/ml, (c) 10 mg/ml, (d) 50 mg/ml, (e) 100 mg/ml shellac and 3.5 mg/ml curcumin. (f) The particle size is linearly proportional to the shellac concentration. Shellac nanoparticles have a negative zeta potential due to the partial ionization of their carboxylic groups. (g) The viscosity of shellac in ethanol increases as its concentration increases. (h) The nanoparticles prepared by microfluidics are more homogeneous than those prepared by bulk mixing.

shellac in ethanol flows along the central channel and is squeezed into a thin stream by the outer water phase flowing at a higher flow rate. The narrow width of the focused stream enables a fast diffusion and rapid mixing of ethanol with water. Therefore, curcumin co-precipitates with shellac, forming curcumin-loaded nanoparticles, as shown by the SEM images in Fig. 1b-e. The dispersion of these nanoparticles in water prepared by the one-step green process is readily edible, transparent and colorful, which is ideal for various applications.

The size of shellac nanoparticles can be tuned in a wide range from tens of nanometers to hundreds of nanometers by varying the concentration of shellac in ethanol; the particle size increases almost linearly from d~55 nm to d~188 nm when the shellac concentration increases from 10 mg/ml to 100 mg/ml, as shown by the dynamic light scattering measurements in Fig. 1f. The nanoparticles are more homogeneous than those prepared by bulk mixing, as shown in Fig. 1h. All the nanoparticles have a negative zeta potential of ~62 mV, due to ionized carboxylic groups at the surface.[30] Interestingly, the measured viscosity of shellac in ethanol also shows a linear dependence on the shellac concentration, as shown in Fig. 1g and Fig. S3. The consistent increase in nanoparticle size with an increase in polymer concentration and solution viscosity is consistent with the self-assembly of nanoparticles under rapid mixing, i.e. solvent exchange is complete before polymers begin to aggregate ($\tau_{mix} < \tau_{agg}$) and the particle size is determined by the growth in a characteristic aggregation time through a diffusion-limited process, thus limited by the concentration and viscosity of the polymer solution.[31]

Controlled co-precipitation of curcumin and shellac by rapid mixing in microfluidic channels.

Fluid dynamic simulations are performed to understand the detailed diffusion and mixing process of ethanol and water within the microfluidic device, as shown in Fig. 2a and b. The Reynolds number in the microfluidic channels is typically low, around 39, and the diffusion of ethanol into water across the laminar flow is generally slow, on the order of second.[32] However, the hydrodynamic flow focusing is advantageous to shear the central flow into a thin stream and form laminar vortices.[33] Therefore, in addition to molecular diffusion, the mixing in the microfluidic device is greatly enhanced by the hydrodynamic flow focusing, which engulfs the inner fluid, forming partially segregated laminates, as modelled in Fig. 2d-f and discussed in detail in Discussion S1. With a typical experimental value of Q_{in}=0.5 ml/h and Q_{out}=20 ml/h, the calculated eddy diffusion coefficient is ε_D~8.1x10^{-6} m^2/s, which is three orders larger than the molecular diffusion coefficient

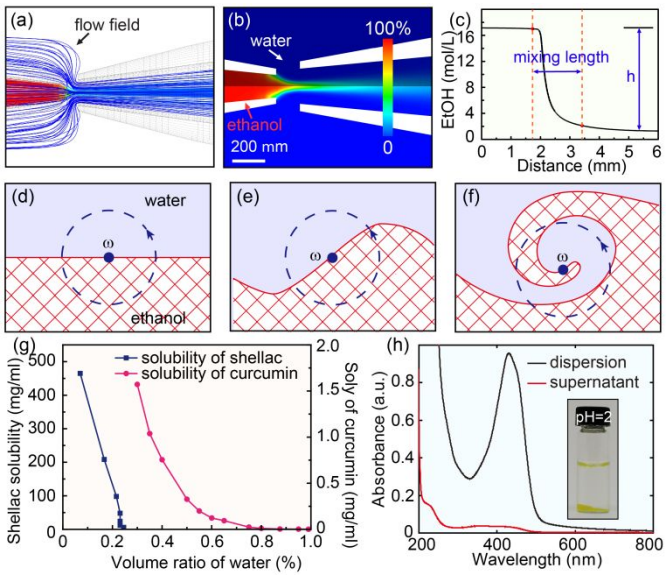

Fig. 2 Controlled co-precipitation of curcumin and shellac by rapid mixing in microfluidic channels. (a) and (b) Fluid dynamic simulation of the flow field and the ethanol concentration gradient, respectively. Q_{in}=0.5 ml/h and Q_{out}=20 ml/h. (c) The mixing length of ethanol and water defined as the length between 99% and 5% of ethanol decrement. (d), (e) and (f) Systematic illustrations showing the evolution of a laminar vortex that engulfs the inner fluid, forming partially segregated laminates, which enhance the mixing process. ω is the angular velocity of the vortex and the dashed circle represents the direction of the flow field. (g) Solubility of shellac (blue curve) and curcumin (red curve) in ethanol/water mixtures. Shellac precipitates before curcumin when the water content increases. (h) UV-Vis absorption of curcumin encapsulated in shellac nanoparticles (black curve) and unencapsulated curcumin left in the supernatant (red curve), suggesting an encapsulation efficiency of 98% for nanoparticles prepared by 50 mg/ml shellac.

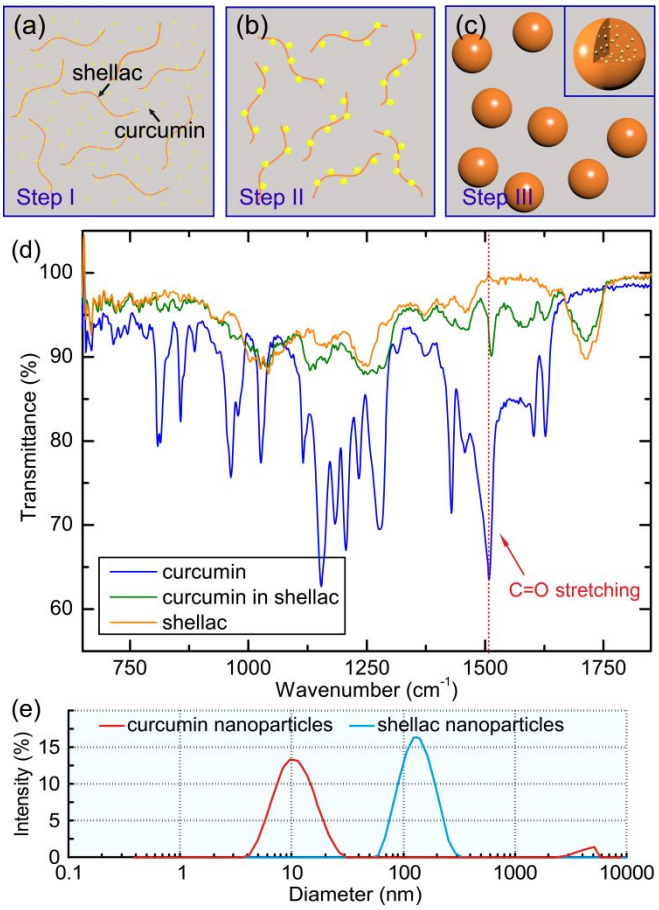

Fig. 3 Effective encapsulation of curcumin in shellac nanoparticles via molecular interactions is achieved through three steps. (a) Curcumin molecules bind to the polymer chains via hydrogen bonding when co-dissolved in ethanol. (b) During the early stage of the co-precipitation process, curcumin first forms nanoaggregates on the polymer chains, due to heterogeneous nucleation and growth. (c) Shellac polymer then precipitates and pulls curcumin nanoaggregates together, forming curcumin-loaded nanoparticles. (d) The FT-IR spectrum of curcumin at 1508.5 cm^{-1} is attributed to its C=O stretching, which shifts to a higher wavenumber when it is dispersed in shellac nanoparticles, suggesting hydrogen bonds between curcumin and shellac. (e) Curcumin nanoaggregates loaded in shellac nanoparticles of d~125 nm have an average size of d~11.8 nm, as revealed by the dynamic light scattering.

D~1.24x10^{-9} m^2/s. The simulated mixing time is τ_{mix}~9 ms with a mixing length of l~1.6 mm (Fig. 2c). This mixing time (τ_{mix}) is shorter than the typical nanoparticle aggregation time (τ_{agg}), which is on the order of tens of milliseconds.[31] The rapid mixing thus offers a unique opportunity to engineering the co-precipitation process of curcumin and shellac.[25]

Effective encapsulation of curcumin in shellac nanoparticles via molecular interactions is achieved through three steps.

If ethanol and water were mixed slowly, shellac would precipitate before curcumin, leading to a failure of curcumin encapsulation. This is because the solubility of shellac decreases dramatically to zero when the water content increases to 22 vol%, while that of curcumin occurs at a much higher water content of 50 vol%, as shown in Fig. 2g. However, the rapid mixing in the microfluidic device ensures that both curcumin and shellac experience a fast change of solvent, leading to their co-precipitation. During the co-precipitation process, embedment of curcumin in the polymer matrix benefits from the hydrophobicity of both curcumin and shellac. However, to achieve an encapsulation efficiency of 96%, 98% and 98% for nanoparticles prepared by 10 mg/ml, 25 mg/ml and 50 mg/ml shellac, respectively (Fig. 2h), which is extremely high as compared to various other nanoparticles,[34-36] we introduce molecular interactions to direct the encapsulation of curcumin in shellac nanoparticles.

We propose that the encapsulation process is achieved through three steps. First, when co-dissolved in ethanol, curcumin molecules bind to the polymer chains via hydrogen bonding and serve as the preferential nucleation sites, as modelled in Fig. 3a. Second, during the early stage of the co-precipitation process, curcumin molecules preferentially aggregate on the polymer chains, due to heterogeneous nucleation and growth, as suggested in Fig. 3b. Third, shellac subsequently pulls all curcumin nanoaggregates together and embeds them in its polymer matrix, forming curcumin-loaded nanoparticles, as shown in Fig. 3c. The molecular interactions between curcumin and shellac are proved by the shifting of the C=O stretching of curcumin measured by the FT-IR experiments. The C=O stretching of curcumin changes from 1508.5 cm^{-1} in neat curcumin to 1513.5 cm^{-1} when dispersed in the nanoparticles due to the hydrogen bonds between the C=O groups of curcumin with the COOH groups of shellac, as shown in Fig. 3d and Fig. S4. The hierarchical structure of curcumin nanoaggregates in shellac nanoparticles is supported by the dynamic light scattering measurement; curcumin nanoaggregates (d~11.8 nm) are roughly 10 times smaller than shellac nanoparticles (d~125 nm), as shown in Fig. 3e. Therefore, molecular interactions play an important role during the co-precipitation process, which efficiently encapsulate

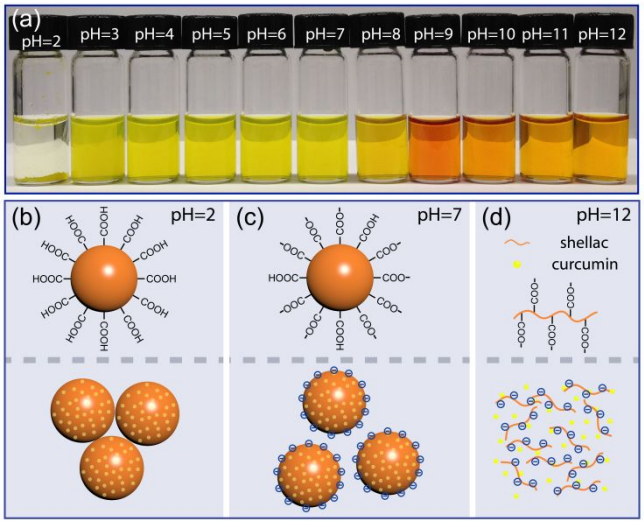

Fig. 4 Stable dispersion of curcumin-loaded shellac nanoparticles over a wide pH range. (a) Dispersity of shellac nanoparticles in water at different pHs. (b) At low pH, e.g. pH=2, the dissociation of H^+ cations from the carboxylic groups of shellac is strongly suppressed and the hydrophobic nature of shellac causes the nanoparticles to aggregate. (c) At neutral pH, shellac nanoparticles are well dispersed in water and stabilized by the electrostatic repulsion. (d) At high pH, e.g. pH=12, shellac nanoparticles are dissolved in water and curcumin is directly exposed to the alkaline condition, as suggested by its orange color.

curcumin nanoaggregates in the polymer matrix, forming hierarchical nanoparticles.

Excellent dispersity of nanoparticles in water over a wide pH range.

Shellac nanoparticles are promising carriers; their dispersion in water is transparent and stable over a wide pH range, as shown in Fig. 4a and Fig. S5. At low pH, e.g. pH=2, most carboxylic groups at the particle surface are protonated and the hydrophobicity of shellac causes the nanoparticles to aggregate and sink, as modelled in Fig. 4b. Over a wide pH range from pH=4 to pH=7, the partial dissociation of the carboxylic groups makes the nanoparticles negatively charged; the electrostatic repulsion between them then prevents the aggregation, as modelled in Fig. 4c. When the average particle size is smaller than d~125 nm, their dispersion in water without any stabilizer shows no observable sedimentation after two months being stationary due to Brownian motion, as shown in Fig. S6. At high pH, e.g. pH=12, the high dissociation rate of the carboxylic groups makes shellac nanoparticles dissolvable in water, as modelled in Fig. 4d. Curcumin is thus directly exposed to the alkaline solution, which is suggested by the shift of its absorption spectrum to higher wavelength and the change of its color from yellow to orange (Fig. S7).[37]

Enhanced stability of curcumin encapsulated in shellac nanoparticles.

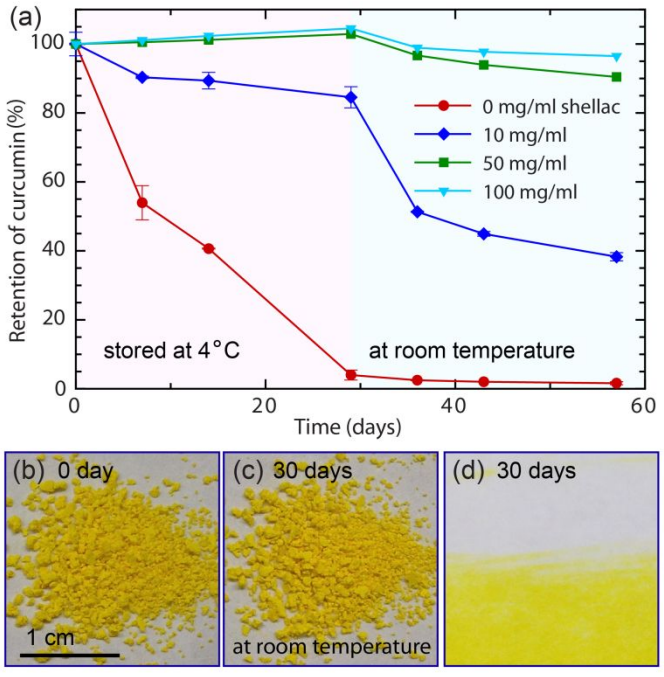

Fig. 5 Enhanced stability of curcumin dispersed in shellac nanoparticles. (a) Retention of curcumin encapsulated in shellac nanoparticles is significantly higher than that directly exposed to ambient conditions. After 29 days, the samples are moved from 4°C to room temperature. (b) and (c) Freeze-dried shellac nanoparticles stored at room temperature show no difference after 30 days, i.e. the shade of yellow color barely changes. (d) Color painting using curcumin-loaded nanoparticles after 30 days.

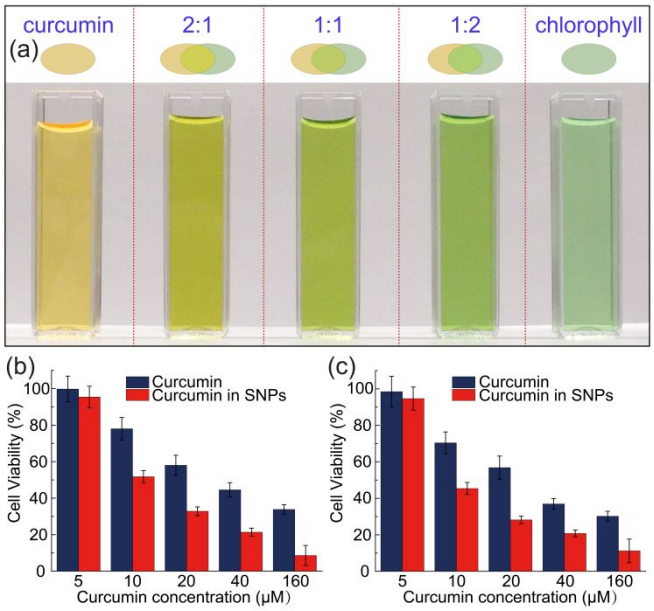

Fig. 6 Biocompatible colorant-loaded shellac nanoparticles for color drinks. (a) Color sequence from yellow to green produced by mixtures of curcumin-loaded and chlorophyll-loaded nanoparticles. Chlorophyll is loaded in shellac nanoparticles following the same procedure. Viability of (b) DLD1 and (c) HT29 cells in the presence of unencapsulated curcumin (blue columns) and curcumin loaded in shellac nanoparticles (red columns), suggesting shellac nanoparticles are effective carriers that improve curcumin's bioavailability.

In addition to dispersing them in water and avoid color staining (Fig. S8), the nanoparticle carriers also protect the colorants from harsh ambient conditions, and provide a favorable microenvironment against degradation. Similar to most natural colorants, curcumin has a very low stability. When proton is removed from its phenolic group, it leads to a rapid hydrolytic degradation of curcumin molecule.[38] However, the carboxylic groups of the polymer matrix could offer protons to curcumin molecules, forming conjugated diene structure and leading to enhanced stability.[39] To prove the enhanced stability of curcumin encapsulated in the nanoparticles, undegraded curcumin is monitored over time using UV-Vis spectroscopy, whose absorption obeys the Beer-Lambert law and is linearly proportional to its concentration, as shown in Fig. S9 and Fig. S10. In the absence of the protection of shellac nanoparticles, most curcumin degrades within 29 days even at 4°C, as shown in Fig. 5a. In contrast, curcumin embedded in the polymer matrix is stable for a long period of time; for example, the sample prepared using 50 mg/ml shellac shows no observable degradation after 29 days at 4°C and less than 10% degradation after another 28 days at room temperature. Dried powder samples also show very good stability performance and there is no observable color change after 30 days stored at room temperature, as shown in Fig. 5b-d.

The one-step preparation of colorant-loaded nanoparticles by co-precipitation in microfluidic channels is versatile. Chlorophyll, for example, a hydrophobic natural colorant that imparts green color to vegetables,[40] could also be encapsulated in shellac nanoparticles following the same procedure. While curcumin-loaded nanoparticles only impart a yellow color, the addition of chlorophyll-loaded nanoparticles could greatly

enrich the color appearance; mixtures of them produce a wide range of colors from yellow, light green to green, as shown in Fig. 6a and Fig. S11. These results suggest that a series of natural colorants could be incorporated in shellac nanoparticles to achieve desired color appearance.

Biocompatible colorant-loaded shellac nanoparticles for color drinks with health benefits.

The use of natural colorant-loaded nanoparticles, such as curcumin-loaded nanoparticles, imparts vivid color to the products and brings very important health benefits. Curcumin is considered by National Cancer Institute as the third generation of cancer chemo-preventive agent in America and daily administration of curcumin provide an alternative strategy to control the initiation and progression of cancer.[41,42] We demonstrate that curcumin-loaded shellac nanoparticles could also improve the bioavailability of curcumin. Shellac nanoparticles are biocompatible and there is no decrease of cell viability of HT-29 and CACO-2 cells cultured in the presence of them, as shown in Fig. S12. When cultured in the dispersion of curcumin-loaded nanoparticles, the viability of carcinogenic DLD1 and HT-29 cells is generally lower than that cultured with unencapsulated curcumin, as shown in Fig. 6b.

Conclusions

We demonstrate that the use of microfluidics to ensure rapid mixing offers a facile way to control the co-precipitation process and tailor the properties of colorant-loaded nanoparticles. The design of molecules interactions could effectively improve the encapsulation efficiency and provide a favorable microenvironment for stability improvement. The developed curcumin-loaded shellac nanoparticles have shown various advantages, including biocompatibility, transparency, controlled particle size, improved particle homogeneity, wide pH stability range, high encapsulation efficiency and enhanced stability, thus representing an important step towards the applications of natural colorants in drinks with appealing color and health benefits. In addition to natural colorants, various actives could easily be loaded in the designed nanoparticles following the same strategy. Therefore, the controlled synthesis of active-loaded nanoparticles by microfluidics also represents a platform for further developments of various functional materials that address the demands of different applications.

Conflicts of interest

There are no conflicts to declare.

Author Contribution

L. K., R. C., Q. C. and M. H. synthesized and characterized the nanoparticles. X. W. performed the simulation. C. Z. did the cell viability test. D. C. designed the experiment. D. C., Z. Y. and D. A W. analysed the data and wrote the paper.

Acknowledgements

This work is supported by the National Natural Science Foundation of China (Grant No. 21878258 and Grant No. 11704331) and the Fundamental Research Funds for the Central Universities (Grant No. 2018QNA4016). This work is also supported by the National Science Foundation (DMR-1310266) and the Harvard Materials Research Science and Engineering Center (DMR-1420570). C.-X. Zhao acknowledges the financial support from the Australian Research Council under Future Fellowship project (FT140100726).

References

1 A. Downham and P. Collins, Int. J. Food Sci. Tech., 2000, **35**, 5-22.
2 M. J. Scotter, *Qual. Assur. Saf. Crops Foods*, 2011, **3**, 28-39.
3 H. Rymbai, R. Sharma and M. Srivasta, *Int. J. Pharmacol. Res.*, 2011, **3**, 2228-2244.
4 G. A. F. Hendry and J. Houghton, *Natural food colorants*, Springer Science & Business Media, Boston, 1996.
5 C. F. Chignell, P. Bilskj, K. J. Reszka, A. G. Motten, R. H. Sik and T. A. Dahl, *Photochem. Photobiol.*, 1994, **59**, 295-302.
6 S. V. Jovanovic, S. Steenken, C. W. Boone and M. G. Simic, *J. Am. Chem. Soc.*, 1999, **121**, 9677-9681.
7 R. Sharma, A. Gescher and W. Steward, *Eur. J. Cancer*, 2005, **41**, 1955-1968.
8 H. Hatcher, R. Planalp, J. Cho, F. Torti and S. Torti, *Cell. Mol. Life Sci.*, 2008, **65**, 1631-1652.
9 J. Ahn, J. Jeong, H. Lee, M. J. Sung, C. H. Jung, H. Lee, J. Hur, J. H. Park, Y. J. Jang and T. Y. Ha, *J. Biomed. Nanotechnol.*, 2017, **13**, 688-698.
10 A. A. Thorat and S. V. Dalvi, *Cryst. Growth Des.*, 2015, **15**, 1757-1770.
11 K. Sou, B. O. Oyajobi, B. Goins, W. T. Phillips and E. Tsuchida, *J. Biomed. Nanotechnol.*, 2009, **5**, 202-208.
12 J. Shaikh, D. Ankola, V. Beniwal, D. Singh and M. R. Kumar, *Eur. J. Pharm. Sci.*, 2009, **37**, 223-230.
13 K. Zhang, P. P. Yang, J. P. Zhang, L. Wang and H. Wang, *Chin. Chem. Lett.*, 2017, **28**, 1808-1816.
14 S. S. Bansal, M. Goel, F. Aqil, M. V. Vadhanam and R. C. Gupta, *Cancer Prev. Res.*, 2011, **4**, 1158-1171.
15 Z. Fang and B. Bhandari, *Trends Food Sci. Technol.*, 2010, **21**, 510-523.
16 L. Li, F. S. Braiteh and R. Kurzrock, *Cancer*, 2005, **104**, 1322-1331.
17 A. Altunbas, S. J. Lee, S. A. Rajasekaran, J. P. Schneider and D. J. Pochan, *Biomaterials*, 2011, **32**, 5906-5914.
18 T. G. Shutava, S. S. Balkundi, P. Vangala, J. J. Steffan, R. L. Bigelow, J. A. Cardelli, D. P. O'Neal and Y. M. Lvov, *Acs Nano*, 2009, **3**, 1877-1885.
19 L. W. Tan, B. Y. Ma, Q. Zhao, L. Zhang, L. J. Chen, J. R. Peng and Z. Y. Qian, *J. Biomed. Nanotechnol.*, 2017, **13**, 393-408.
20 J. M. Lim, A. Swami, L. M. Gilson, S. Chopra, S. Choi, J. Wu, R. Langer, R. Karnik and O. C. Farokhzad, *Acs Nano*, 2014, **8**, 6056-6065.
21 D. Liu, S. Cito, Y. Zhang, C. F. Wang, T. M. Sikanen and H. A. Santos, *Adv. Mater.*, 2015, **27**, 2298-2304.
22 S. S. Datta, A. Abbaspourrad and D. A. Weitz, *Mater Horiz*, 2014, **1**, 92-95.
23 W. Wang, M. J. Zhang and L. Y. Chu, *Acc. Chem. Res.*, 2014, **47**, 373-384.
24 C. X. Zhao, *Adv. Drug Del. Rev.*, 2013, **65**, 1420-1446.
25 R. Karnik, F. Gu, P. Basto, C. Cannizzaro, L. Dean, W. Kyeimanu, R. Langer and O. C. Farokhzad, *Nano Lett.*, 2008, **8**, 2906-2912.

26 D. Liu, H. Zhang, S. Cito, J. Fan, E. M. Mäkilä, J. J. Salonen, J. Hirvonen, T. M. Sikanen, D. A. Weitz and H. A. Santos, *Nano Lett.*, 2017, **17**, 606-614.
27 C. Stoffelen, R. Munirathinam, W. Verboom and J. Huskens, *Mater Horiz*, 2014, **1**, 595-601.
28 H. Weinberger and W. H. Gardner, *Ind.eng.chem*, 1938, **30**, 454-458.
29 D. Chen, E. Amstad, C. X. Zhao, L. Cai, J. Fan, Q. Chen, M. Hai, S. Koehler, H. Zhang and F. Liang, *Acs Nano*, 2017, **11**, 11978-11985.
30 L. L. Kong, E. Amstad, M. T. Hai, X. Y. Ke, D. Chen, C. X. Zhao and D. A. Weitz, *Chin. Chem. Lett.*, 2017, **28**, 1897-1900.
31 B. K. Johnson and R. K. Prud'Homme, *Phys. Rev. Lett.*, 2003, **91**, 118302.
32 L. D. Scampavia, G. Blankenstein, J. Ruzicka and G. D. Christian, *Anal. Chem.*, 1995, **67**, 2743-2749.
33 J. Baldyga and J. R. Bourne, *Chem. Eng. Commun.*, 2007, **28**, 243-258.
34 A. Mukerjee and J. K. Vishwanatha, *Anticancer Res.*, 2009, **29**, 3867-3875.
35 K. Pan, Q. Zhong and S. J. Baek, *J. Agric. Food Chem.*, 2013, **61**, 6036-6043.
36 A. Sahu, N. Kasoju, P. Goswami and U. Bora, *J. Biomater. Appl.*, 2011, **25**, 619-639.
37 Y. Erez, R. Simkovitch, S. Shomer, R. Gepshtein and D. Huppert, *J. Phys. Chem. A*, 2014, **118**, 872-884.
38 T. Esatbeyoglu, K. Ulbrich, C. Rehberg, S. Rohn and G. Rimbach, *Food Funct.*, 2015, **6**, 887-893.
39 Y. J. Wang, M. H. Pan, A. L. Cheng, L. I. Lin, Y. S. Ho, C. Y. Hsieh and J.-K. Lin, *J. Pharm. Biomed. Anal.*, 1997, **15**, 1867-1876.
40 A. L. İnanç, *Academic Food Journal*, 2011, **9**, 26-23.
41 S. Bisht, M. Mizuma, G. Feldmann, N. A. Ottenhof, S.-M. Hong, D. Pramanik, V. Chenna, C. Karikari, R. Sharma and M. G. Goggins, *Mol. Cancer Ther.*, 2010, **9**, 2255-2264.
42 Y. J. Surh, *Nat. Rev. Cancer*, 2003, **3**, 768-780.

Table of content

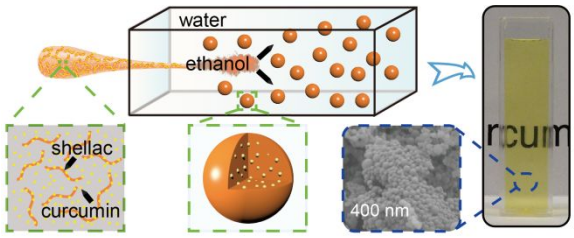

Controlled co-precipitation of biocompatible colorant-loaded nanoparticles in microfluidic channels for natural color drinks.